Inorg. Chem. **2003**, *42*, 5604–5611

Pendant Macrocyclic Metallic Building Blocks for the Design of Cyano-Bridged Heterometallic Complexes with 1D Chain and 2D Layer Structures

Hui-Zhong Kou,*,† Bei Chuan Zhou,† Song Gao,‡ Dai-Zheng Liao,§ and Ru-Ji Wang†

Department of Chemistry, Tsinghua University, Beijing 100084, P. R. China, State Key Laboratory of Rare Earth Materials Chemistry and Applications, Peking University, Beijing 100871, P. R. China, and Department of Chemistry, Nankai University, Tianjin 300071, P. R. China

Received January 13, 2003

A series of cyano-bridged Ni(II)–Cr(I/III) complexes have been synthesized by the reactions of hexaazacyclic Ni^{II} complexes with $[Cr(CN)_6]^{3-}$ or $[Cr(CN)_5(NO)]^{3-}$. Using the tetravalent Ni^{II} complex $[Ni(H_2L^2)]^{4+}$ (L^2 = 3,10-bis(2-aminoethyl)-1,3,6,8,10,12-hexaazacyclotetradecane), one-dimensional chainlike complexes were produced and subject to magnetic studies, affording the intermetallic magnetic exchange constants of $J_1 = +0.23$ cm^{-1} and $J_2 = +8.4$ cm^{-1} for the complex $[Ni(H_2L^2)][Cr(CN)_5(NO)]ClO_4 \cdot 5H_2O$ (**1**) and of $J = +5.9$ cm^{-1} for the complex $[Ni(H_2L^2)]_4[Cr(CN)_6]_5OH \cdot 15H_2O$ (**2**). X-ray diffraction analysis shows that complex **1** has a zigzag chain structure, whereas complex **2** consists of a branched chain structure. Complex **2** exhibits antiferromagnetic ordering at 8.0 K (T_N). When an octahedral Ni^{II} complex *cis*-$[NiL^3(en)]^{2+}$ (en = 1,2-ethylenediamine, L^3 = 3,10-bis(2-hydroxyethyl)-1,3,5,8,10,12-hexaazacyclotetradecane) was used for the synthesis, the common 2D honeycomb-layered complex $[NiL^3]_3[Cr(CN)_5(NO)]_2 \cdot 8H_2O$ (**3**) was obtained, which has a T_N value of 3.3 K. Below T_N, a metamagnetic behavior was observed in complexes **2** and **3**.

Introduction

Recently, cyano-bridged complexes based on hexacyanometalate have been extensively investigated in the search for room-temperature molecular magnets and for the understanding of magneto−structural relationships.[1−23] Among these, two-dimensional honeycomblike complexes $[NiL]_3[M(CN)_6]_2 \cdot nH_2O$ (L = polyazamacrocyclic ligands) have

* To whom correspondence should be addressed. E-mail: kouhz@mail.tsinghua.edu.cn. Fax: 86-10-62788765.

† Tsinghua University.

‡ Peking University.

§ Nankai University.

(1) (a) Sato, O.; Iyoda, T.; Fujishima. A.; Hashimoto, K. *Science* **1996**, *272*, 704. (b) Holmes, S. M.; Girolami, G. S. *J. Am. Chem. Soc*. **1999**, *121*, 5593. (c) Ferlay, S.; Mallah, T.; Ouahe's, R.; Veillet, P.; Verdaguer, M. *Inorg. Chem.* **1999**, *38*, 229. (d) Mallah, T.; Thiebaut, S.; Verdaguer, M.; Veillet, P. *Science* **1993**, *262*, 1554.

(2) Langenberg, K. V.; Batten, S. R.; Berry, K. J.; Hockless, D. C. R.; Moubaraki, B.; Murray, K. S. *Inorg. Chem*. **1997**, *36*, 5006.

(3) El Fallah, M. S.; Rentschler, E.; Caneschi, A.; Sessoli, R.; Gatteschi, D. *Angew. Chem., Int. Ed. Engl*. **1996**, *35*, 1947.

(4) Smith, J. A.; Galan-Mascaros, J.-R.; Clerac, R.; Dunbar, K. R. *Chem. Commun*. **2000**, 1077.

(5) Mondal, N.; Saha, M. K.; Bag, B.; Mitra, S.; Gramlich, V.; Ribas, J.; El Fallah, M. S. *J. Chem. Soc., Dalton Trans*. **2000**, 1601.

(6) Ohba, M.; Usuki, N.; Fukita, N.; Okawa, H. *Angew. Chem., Int. Ed*. **1999**, *38*, 1795. Ohba, M.; Okawa, H.; Fukita, N.; Hashimoto, Y. *J. Am. Chem. Soc*. **1997**, *119*, 1011. Ohba, M.; Maruone, N.; Okawa, H.; Enoki, T.; Latour, J.-M. *J. Am. Chem. Soc*. **1994**, *116*, 11566.

(7) Parker, R. J.; Hockless, D. C.; Moubaraki, B.; Murray, K. S.; Spiccia, L. *Chem. Commun*. **1996**, 2789. Parker, R. J.; Spiccia, L.; Batten, S. R.; Cashion, J. D.; Fallon, G. D. *Inorg. Chem.* **2001**, *40*, 4696. Parker, R. J.; Spiccia, L.; Moubaraki, B.; Murray, K. S.; Hockless**,** D. C. R.; Rae, A. D.; Willis, A. C. *Inorg. Chem.* **2002**, *41*, 2489. Parker, R. J.; Spiccia, L.; Berry, K. J.; Fallon, G. D.; Moubaraki, B.; Murray, K. S. *Chem. Commun.* **2001,** 333.

(8) (a) Miyasaka, H.; Matsumoto, N.; Okawa, H.; Re, N.; Gallo, E.; Floriani, C. *Angew. Chem., Int. Ed. Engl.* **1995**, *34*, 1446. (b) Miyasaka, H.; Matsumoto, N.; Okawa, H.; Re, N.; Gallo, E.; Floriani, C. *J. Am. Chem. Soc.* **1996**, *118*, 981. (c) Re, N.; Gallo, E.; Floriani, C.; Miyasaka, H.; Matsumoto, N. *Inorg. Chem.* **1996**, *35*, 6004. (d) Miyasaka, H.; Matsumoto, N.; Re, N.; Gallo, E.; Floriani, C. *Inorg. Chem.* **1997**, *36*, 670.

(9) Kou, H.-Z.; Gao, S.; Zhang, J.; Wen, G.-H.; Su, G.; Zheng, R. K.; Zhang, X. X. *J. Am. Chem. Soc.* **2001**, *123*, 11809.

(10) Thétiot, F.; Triki, S.; Pala, J. S.; Gómez-García, C. J.; Golhen, S. *Chem. Commun.* **2002**, 1078.

(11) Coronado, E.; Gomez-Garcia, C. J.; Nuez, A.; Romero, F. M.; Rusanov, E.; Stoeckli-Evans, H. *Inorg. Chem*. **2002**, *41*, 4615.

(12) (a) Marvillers, A.; Parsons, S.; Riviere, E.; Audiere, J.-P.; Mallah, T. *Chem. Commun*. **1999**, 2217. (b) Rogez, G.; Parsons, S.; Villar, V.; Mallah, T. *Inorg. Chem.* **2001**, *40*, 3836. (c) Scuiller, A.; Mallah, T.; Nivorozkhin, A.; Tholence, J.-L.; Verdaguer, M.; Veillet, P. *New J. Chem*. **1996**, *20*, 1.

(13) Vostrikova, K. E.; Luneau, D.; Wernsdorfer, W.; Rey, P.; Verdaguer, M. *J. Am. Chem. Soc*. **2000**, *122*, 718.

10.1021/ic034028y CCC: $25.00
Published on Web 07/29/2003

Chart 1

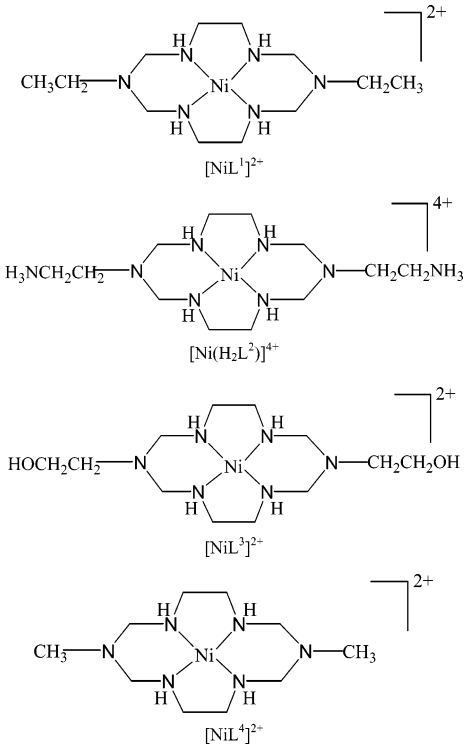

been prepared by the reaction of $[M(CN)_6]^{3-}$ (M = Fe, Cr, Mn) with four-coordinate macrocyclic Ni(II) complexes.[16−22] Also, the two-dimensional brick wall-like complex $[NiL^1]_3[Fe(CN)_6]_2\cdot 6H_2O$ (L^1 = 3,10-diethyl-1,3,5,8,10,12-hexaazacyclotetradecane) has been reported,[22] which exhibits a large coercive field of 1500 Oe. Using a hexaazamacrocyclic Ni(II) building block with four positive charges, $[Ni(H_2L^2)](ClO_4)_4$ (Chart 1), we have prepared novel pentanuclear and one-dimensional Ni(II)−Fe(III) complexes via the reaction of $K_3[Fe(CN)_6]$ with $[Ni(H_2L^2)](ClO_4)_4$.[23] Herein, we present the synthesis, structural characterization, and magnetic properties of the novel one-dimensional complexes incorporating $[Cr(CN)_6]^{3-}$ or $[Cr(CN)_5(NO)]^{3-}$ and $[Ni(H_2L^2)]^{4+}$.

Experimental Section

Elemental analyses of carbon, hydrogen, and nitrogen were carried out with an Elementar Vario EL. The infrared spectroscopy was performed on a Magna-IR 750 spectrophotometer in the 4000−650 cm^{-1} region. Variable-temperature magnetic susceptibility measurements of **1** and **2** were performed on a Quantum Design MPMS SQUID magnetometer. Magnetic susceptibility measurements of **3** and zero-field ac magnetic susceptibility and field dependence of magnetization measurements of **2** were on a MagLab 2000 magnetometer. The experimental susceptibilities were corrected for the diamagnetism of the constituent atoms (χ_d = -3.0×10^{-4} emu mol^{-1} for **1**, -9.7×10^{-4} emu mol^{-1} for **2**, and -6.5×10^{-4} emu mol^{-1} for **3**) (Pascal's tables).

Syntheses. The precursors $[Ni(H_2L^2)](ClO_4)_4$,[24] $[NiL^3(en)Ni(en)_3](ClO_4)_4$,[25] $K_3[Cr(CN)_6]$,[26] and $K_3[Cr(CN)_5(NO)]\cdot H_2O$[27] were prepared by the literature methods.

$[Ni(H_2L^2)][Cr(CN)_5(NO)]ClO_4\cdot 5H_2O$ (1). Yellow single crystals of **1** suitable for X-ray structure analysis were grown at room temperature by the slow evaporation of a yellow MeCN−H_2O (1:10 v/v) solution (15 mL) of $[Ni(H_2L^2)](ClO_4)_4$ (0.1 mmol, 74.7 mg) and $K_3[Cr(CN)_5(NO)]\cdot H_2O$ (0.1 mmol, 32.9 mg). Yield: 15 mg (10%). IR (cm^{-1}): ν(C≡N), 2111 s, 2120 sh, ν(N≡O), 1675 vs, ν(Cl−O), 1101 br. Anal. Calcd for $C_{17}H_{44}N_{14}O_{10}ClNiCr$: C, 27.20; H, 5.91; N, 26.12. Found: C, 27.3; H, 6.0; N, 26.2.

$[Ni(H_2L^2)]_4[Cr(CN)_6]_5OH\cdot 15H_2O$ (2). Yellow single crystals of **2** suitable for X-ray structure analysis were grown at room temperature by the slow diffusion of a yellow MeCN solution (5 mL) of $[Ni(H_2L^2)](ClO_4)_4$ (0.1 mmol, 74.7 mg) into a yellow aqueous solution (5 mL) of $K_3[Cr(CN)_6]\cdot H_2O$ (0.1 mmol, 34.3 mg). Yield: 24 mg (9%). IR (cm^{-1}): ν(C≡N), 2153 sh, 2127 vs. Anal. Calcd for $C_{78}H_{167}N_{62}O_{16}Ni_4Cr_5$: C, 34.39; H, 6.18; N, 31.88. Found: C, 35.2; H, 6.1; N, 31.7.

$[NiL_3]_3[Cr(CN)_5(NO)]_2\cdot 8H_2O$ (3). Well-shaped yellow single crystals of the complex were obtained by slow diffusion of a pale purple $[NiL^3(en)Ni(en)_3](ClO_4)_4$ (0.1 mmol, 104.5 mg) solution in MeCN (10 mL) into a yellow aqueous solution (10 mL) of $K_3[Cr(CN)_5(NO)]\cdot H_2O$ (0.1 mmol, 32.9 mg) at room temperature for several weeks. Yield: 16 mg (10%). IR (cm^{-1}): ν(C≡N), 2142 s, 2111 s; ν(O≡N) 1670 vs. Anal. Calcd for $C_{46}H_{106}Cr_2N_{30}Ni_3O_{16}$: C, 34.20; H, 6.61; N, 26.01. Found: C, 34.4; H, 6.4; N, 26.3.

X-ray Structure Determination. The data collections for **1** and **3** were done on a Rigaku R-Axis RIPID IP (173 K), and that of **2** was done on a Bruker Smart CCD (293 K) diffractometer. The structures were solved by direct method SHELXS-97 and refined by full-matrix least-squares (SHELXL-97) on F^2. Hydrogen atoms were added geometrically and refined using a riding model. The ligand L^3 in complex **3** experienced disorder over two positions. The occupancy factors of two sets of disordered atoms were 0.5. The crystal data are summarized in Table 1.

Results and Discussion

Synthesis and Physical Characterization. The 1D complexes (**1** and **2**) were synthesized by the reaction of

(14) Figuerola, A.; Diaz, C.; El Fallah, M. S.; Ribas, J.; Maestro, M.; Mahia, J. E. *Chem. Commun.* **2001**, 1204. Kou, H.-Z.; Gao, S.; Sun, B.-W.; Zhang, J. *Chem. Mater*. **2001**, *13*, 1431. Kou, H.-Z.; Gao, S.; Jin, X. *Inorg. Chem*. **2001**, *40*, 6295. Hulliger, F.; Landolt, M.; Vetsch, H. *J. Solid State Chem*. **1976**, *18*, 283. Kou, H.-Z.; Gao, S.; Li, C.-H.; Liao, D.-Z.; Zhou, B. C.; Wang, R.-J.; Li. Y.-D. *Inorg. Chem*. **2002**, *41*, 4756.

(15) Yan, B.; Chen, Z. D.; Wang, S. X. *Transition Met. Chem*. **2001**, *26*, 287. Yan, B.; Chen, Z. D.; Wang, S. X.; Gao, S. *Chem. Lett.* **2001**, 350.

(16) Ferlay, S.; Mallah, T.; Vaissermann, J.; Bartolome, F.; Veillet, P.; Verdaguer, M. *J. Chem. Soc., Chem. Commun*. **1996**, 2481.

(17) Colacio, E.; Dominguez-Vera, J. M.; Ghazi, M.; Kivekas, R.; Lloret, F.; Moreno, J. M.; Stoeckli-Evans, H. *Chem. Commun.* **1999**, 987. Colacio, E.; Ghazi, M.; Stoeckli-Evans, H.; Lloret, F.; Moreno, J.-M.; Perez, C. *Inorg. Chem.* **2001**, *40*, 4876. Shen, Z.; Zuo, J. L.; Shi, F. N.; Xu, Y.; Song, Y.; You, X. Z.; Raj, S. S. S.; Fun, H. K.; Zhou, Z. Y.; Che, C. M. *Transition Met. Chem*. **2001**, *26*, 345.

(18) Xiang, H.; Gao, S.; Lu,T. B.; Luck, R. L.; Mao, Z. W.; Chen, X. M.; Ji, L. N. *New J. Chem.* **2001**, *25*, 875.

(19) (a) Kou, H.-Z.; Gao, S.; Bu, W.-M.; Liao, D.-Z.; Ma, B.-Q.; Jiang, Z.-H.; Yan, S.-P.; Fan, Y.-G.; Wang, G.-L. *J. Chem. Soc., Dalton Trans*. **1999**, 2477. (b) Kou, H.-Z.; Bu, W.-M.; Gao, S.; Liao, D.-Z.; Jiang, Z.-H.; Yan, S.-P.; Fan, Y.-G.; Wang, G.-L. *J. Chem. Soc., Dalton Trans*. **2000**, 2996.

(20) Marvilliers, A.; Parsons, S.; Riviere, E.; Audiere, J. P.; Kurmoo, M.; Mallah, T. *Eur. J. Inorg. Chem*. **2001**, 1287.

(21) Kou, H.-Z.; Gao, S.; Bai, O.; Wang, Z.-M. *Inorg. Chem.* **2001**, *40*, 6287.

(22) Kou, H.-Z.; Gao, S.; Ma, B.-Q.; Liao, D.-Z. *Chem. Commun*. **2000**, 1309.

(23) Kou, H.-Z.; Zhou, B. C.; Liao, D.-Z.; Wang, R.-J.; Li, Y.-D. *Inorg. Chem.* **2002**, *41*, 6887.

(24) Kang, S. G.; Ryu, K.; Jung, S.-K.; Kim, J. *Inorg. Chim. Acta* **1999**, *293*, 140.

(25) Xiang, H.; Lu, T. B.; Chen, S.; Mao, Z. W.; Feng, X. L.; Yu, K. B. *Polyhedron* **2001**, *20*, 313.

(26) Cruser, F. V. D.; Miller, E. H. *J. Am. Chem. Soc*. **1906**, *28*, 1132.

(27) Griffith, W. P.; Lewis, J.; Wilkinson, G. *J. Chem. Soc*. **1959**, 872.

Table 1. Crystallographic Data for Complexes **1**−**3**

	1	**2**	**3**
formula	$C_{17}H_{44}ClCrN_{14}NiO_{10}$	$C_{78}H_{167}N_{62}O_{16}Ni_4Cr_5$	$C_{46}H_{106}Cr_2N_{30}Ni_3O_{16}$
fw	750.82	2724.58	1615.74
T/K	173	293	173
space group	$P2_1/c$	$P1$	$P\bar{3}$
a/Å	12.313(2)	14.404(3)	14.856(2)
b/Å	19.448(4)	15.514(3)	14.856(2)
c/Å	15.379(3)	18.147(4)	9.195(2)
α/deg	90	78.02(3)	90
β/deg	109.36(3)	75.65(3)	90
γ /deg	90	63.45(3)	120
V/Å^3	3474.5(11)	3492.3(12)	1757.5(5)
Z	4	1	1
ρ_{calcd}/g cm^{-3}	1.435	1.295	1.527
μ(Mo Kα)/mm^{-1}	0.994	0.971	1.171
data/restraints/params	6043/0/408	12160/0/774	1506/0/182
R1 [$I > 2\sigma(I)$]	0.0566	0.0941	0.0444
wR2 (all data)	0.1395	0.174	0.1142

$[Ni(H_2L^2)](ClO_4)_4$ with $K_3[Cr(CN)_6]$ or $K_3[Cr(CN)_5(NO)]$. As previously indicated, it is anticipated that the reaction of the tetravalent Ni(II) macrocyclic building block with $[Fe(CN)_6]^{3-}$ would result in the 1D chainlike complex rather than the common 2D honeycomblike complexes.[23] However, the chains of **1** and **2** are quite different: that of **1** can be described as zigzag chains similar to that of the 1D NiFe complex,[23] and that of **2** is a branched chain structure.

As aforementioned, there are a number of reports on reactions between square-planar Ni(II) macrocyclic complexes and $[Fe(CN)_6]^{3-}$, $[Cr(CN)_6]^{3-}$, or $[Cr(CN)_5(NO)]^{3-}$. The *cis*-$[NiL^3(en)]^{2+}$ unit in $[NiL^3(en)][Ni(en)_3](ClO_4)_4$ is folded so that the coordination geometry around the Ni(II) ion is similar to that of the *cis*-$[M(L')_2]^{n+}$ (M = Mn, Ni, or Co; L′ stands for bidentate ligands) units.[2,13,28] With the consideration that the reactions of *cis*-$[M(L')_2]^{n+}$ units with hexacyanometalate building blocks always generate magnetic clusters,[2,13,28] we attempted to synthesize clusters by reacting the *cis*-$[NiL^3(en)]^{2+}$ cation with $[Cr(CN)_5(NO)]^{3-}$ and $[Cr(CN)_6]^{3-}$ anion but unexpectedly obtained the honeycomblike coordination polymers $[NiL^3]_3[Cr(CN)_5(NO)]_2\cdot 8H_2O$ and $[NiL^3]_3[Cr(CN)_6]_2\cdot 6H_2O$[22] in which $[NiL^3]^{2+}$ adopts the trans-configuration. Similar results were also observed in the reaction of purple *cis*-$[NiL^4(en)]^{2+}$ (L^4 = 3,10-dimethyl-1,3,5,8,10,12-hexaazacyclotetradecane) with $K_3[Cr(CN)_6]$, which leads to the honeycomblike complex $[NiL^4]_3[Cr(CN)_6]_2\cdot 10H_2O$,[22] as determined by X-ray diffraction analysis.

It may be due to the fact that the *cis*-$[NiL^3(en)]^{2+}$ exists in solution as an equilibrium mixture of square-planar $[NiL^3]^{2+}$, *trans*- and *cis*-$[NiL^3(H_2O)_2]^{2+}$, and *cis*-$[NiL^3(en)]^{2+}$ species.[25] The 2D Ni_3Cr_2 complexes containing the *trans*-$[NiL^3]^{2+}$ units are the only products under the present reaction conditions. Actually, the steric hindrance of the macrocyclic ligands around the Ni(II) ion may be responsible for the formation of the 2D complexes rather than polynuclear clusters.

Table 2. Selected Bond Distances (Å) and Angles (deg) for **1**[a]

Ni1−N9	2.049(5)	Ni1−N7	2.069(4)
Ni1−N8	2.082(4)	Ni1−N10	2.070(5)
Ni1−N4	2.065(5)	Ni1−N1$^{\#1}$	2.110(5)
Cr1−C1	2.063(6)	Cr1−C2	2.002(8)
Cr1−C3	2.032(7)	Cr1−C4	2.093(7)
Cr1−C5	2.045(8)	Cr1−N6	1.707(5)
O1−N6	1.209(6)	N2−C2	1.160(8)
N3−C3	1.161(8)	N4−C4	1.138(7)
N5−C5	1.158(8)	C1−N1	1.141(6)
C4−N4−Ni1	169.9(5)	C1$^{\#1}$−N1$^{\#1}$−Ni1	153.6(5)

[a] Symmetry transformation used to generate equivalent atoms: #1, x, $-y + 3/2$, $z - 1.2$.

Table 3. Selected Bond Distances (Å) and Angles (deg) for **2**

Ni1−N4	2.052(8)	Ni1−N27	2.058(7)
Ni1−N26	2.075(6)	Ni2−N22	2.068(6)
Ni2−N23	2.071(8)	Ni2−N5	2.128(7)
Ni3−N1	2.141(7)	Ni3−N7	2.096(7)
Ni3−N17	2.023(9)	Ni3−N16	2.070(8)
Ni3−N19	2.044(8)	Ni3−N20	2.035(10)
C4−N4−Ni1	175.7(7)	C5−N5−Ni2	162.9(8)
C7−N7−Ni3	169.4(11)	C1−N1−Ni3	155.5(8)

Table 4. Selected Bond Lengths (Å) and Angles (deg) for **3**[a]

Ni1−N2	2.063(4)	Cr1−C2	2.041(5)
Ni1−N3A	2.044(8)	Cr1−N/C1	1.920(7)
Ni1−N3B	2.059(8)	O−N	1.176(9)
Ni1−N4A	2.086(8)	N1−C1	1.176(9)
Ni1−N4B	2.072(7)	N2−C2	1.138(6)
C1$^{\#1}$−Cr1−N	97.7(2)	C1$^{\#2}$−Cr1−C2	88.9(2)
C1$^{\#1}$−Cr1−C2	88.4(2)	C2−Cr1−C2$^{\#2}$	84.23(19)
N−Cr1−C2	170.3(2)	C2−N2−Ni1	167.2(4)

[a] Symmetry transformations used to generate equivalent atoms: #1, $-x + y + 1$, $-x + 1$, z; #2 $-y + 1$, $x - y$, z.

The IR spectra of **1**−**3** exhibit several cyano stretching absorptions between 2000 and 2200 cm^{-1}, suggesting the presence of bridging and nonbridging cyano ligands in $[Cr(CN)_6]^{3-}$ or $[Cr(CN)_5(NO)]^{3-}$. The peaks with higher wavenumber can be assigned to the bridging C≡N stretching mode, while those with low wavenumbers are due to the nonbridging C≡N stretching vibration.[1−23] The strong peak at 1675 cm^{-1} is observed for the $[Cr(CN)_5(NO)]^{3-}$ complexes, which can be assigned to the N≡O stretching vibration.[29] The strong broad peaks centered at the 1100 cm^{-1} indicate the presence of free ClO_4^- anions in complex **1**.

Crystal Structures. Selected bond distances and angles for complexes **1**−**3** are listed in Tables 2−4. The structure of $[Ni(H_2L^2)][Cr(CN)_5(NO)]ClO_4\cdot 5H_2O$ (**1**) consists of a one-dimensional cationic polymer $\{[Ni(H_2L^2)][Cr(CN)_5(NO)]\}_n^{n+}$, with ClO_4^- as the counteranion (Figure 1). The zigzag chain is made of a cyano-bridged alternating $[Cr(CN)_5(NO)]^{3-}$ and $[Ni(H_2L^2)]^{4+}$ fragments. Similar to the 1D $[Fe(CN)_6]^{3-}$-$[Ni(H_2L^2)]^{4+}$ complex,[23] $[Cr(CN)_5(NO)]^{3-}$ uses two *cis*-CN^- groups to connect two $[Ni(H_2L^2)]^{4+}$ groups, whereas each $[Ni(H_2L^2)]^{4+}$ group is linked to two $[Cr(CN)_5(NO)]^{3-}$ ions in trans positions. Two nitrogen atoms of the bridging C≡N ligands coordinate to the Ni(II) ions with the Ni−N contacts of 2.065(5) Å for Ni(1)−N4 and 2.110(5) Å for Ni1−N1$^{\#1}$, respectively. The bridging cyanide ligands

(28) Smith, J. A.; Galan-Mascaros, J. R.; Clerac, R.; Sun, J. S.; Ouyang, X.; Dunbar, K. R. *Polyhedron* **2001**, *20*, 1727. Berlinguette, C. P.; Smith, J. A.; Galan-Mascaros, J. R.; Dunbar, K. R. *C. R. Chim.* **2002**, *5*, 665.

(29) Gans, P.; Sabatini, A.; Sacconi, L. *Inorg. Chem.* **1966**, *5*, 1877.

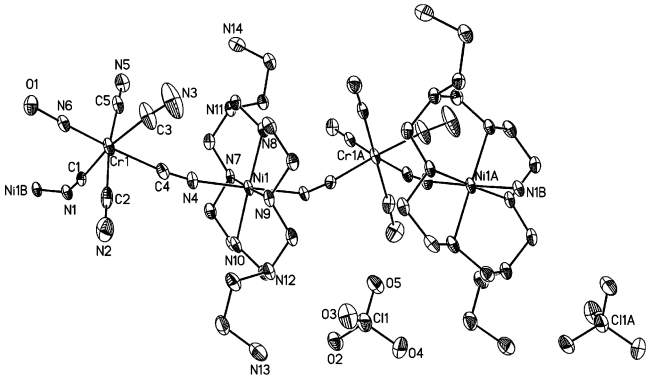

Figure 1. ORTEP diagram of complex **1**, $[Ni(H_2L^2)][Cr(CN)_5(NO)]ClO_4 \cdot 5H_2O$, with thermal ellipsoids at 30% probability.

coordinate to the Ni(II) ions in a bent fashion with the Ni−N≡C bond angles of 153.6(5) and 169.9(5)°, similar to that of the $[Fe(CN)_6]^{3-}$−$[Ni(H_2L)]^{4+}$ complex.[23] The Cr−C bond distances range from 2.002(8) to 2.093(7) Å, and the Cr−N distance is 1.707(5) Å. These data are in good agreement with the reported data for pentacyanonitrosylchromate(I) complexes.[30] The adjacent Cr---Ni distances are 5.252(1) Å for Cr1---Ni1 and 5.127(1) Å for Cr1---Ni1$^{\#1}$.

The shortest interchain metal−metal distance is 6.87 Å for Cr---Ni. Figure 2 shows the intermolecular contacts (N---N = 2.873 Å) between the cyano nitrogen atoms of one chain and the $-NH_3^+$ groups of adjacent chains. The perchlorate anions are situated between the ammonium ends of each $[Ni(H_2L^2)]^{4+}$ portion of the 1D chains. The H-bonded chains form a 3D network and 1D channels along the *c* axis. The interstitial water molecules are situated within the 1D channels (Figure 2).

X-ray crystallography reveals that the structure of $[Ni(H_2L^2)]_4[Cr(CN)_6]_5OH \cdot 15H_2O$ (**2**) consists of a cationic infinite chain with the repeating unit of $\{[Ni(H_2L^2)]_4[Cr(CN)_6]_4\}_n^{4n+}$ and one free $[Cr(CN)_6]^{3-}$ and one OH^- as the counterions. Alternatively, one of the $[Ni(H_2L^2)]^{4+}$ group in the Ni_4Cr_5 unit might be deprotonated and exists as $[Ni(HL^2)]^{3+}$. If so, the formula should be written as $[Ni(HL^2)][Ni(H_2L^2)]_3[Cr(CN)_6]_5 \cdot 16H_2O$. Nevertheless, any assignment does not affect the results of magnetic studies. As shown in Figure 3, in the chain one of the $[Cr(CN)_6]^{3-}$ units (Cr1) uses three *fac*-CN^- groups to connect with three *trans*-$[Ni(H_2L^2)]^{4+}$ groups, whereas the three remaining CN^- groups are monodentate; another $[Cr(CN)_6]^{3-}$ unit (Cr2) uses only one cyano ligand to chelate the nickel(II) ion (Ni3) with the other five cyano ligands intact. Each $[Ni(H_2L^2)]^{4+}$ group is linked to two $[Cr(CN)_6]^{3-}$ ions in trans positions. Four secondary amine nitrogen atoms of the macrocycle coordinate to the nickel center with an average Ni−N distance of 2.066(7) Å for Ni1, 2.069(9) Å for Ni2, and 2.046(9) Å for Ni3. Two nitrogen atoms of the bridging C≡N ligands axially coordinate to the Ni(II) ions with the Ni−N contacts of 2.052(8) Å for Ni1, 2.128(7) Å for Ni2, and 2.083(8) Å (average value) for Ni3, respectively. The bridging cyanide ligands coordinate to the Ni(II) ions mostly in a bent fashion with the Ni−N≡C bond angles ranging from 155.5(8) to 169.4(11)° with the exception of linear Ni1−N4−C4 [175.7(7)°]. The adjacent Cr---Ni distances are 5.217(2) Å for Cr1---Ni1, 5.258(2) Å for Cr1---Ni2, 5.201(2) Å for Cr1---Ni3, and 5.272(2) Å for Cr2---Ni3, respectively. The Cr−C distances range from 2.013(12) to 2.097(15) Å. The branched chain topology can be described as a cyano-bridged zigzag −Ni1−Cr1−Ni2− chain with cyano-bridged −Ni3−Cr2 pendants or as chains with alternating Cr2−Ni3−Cr1< trimers and −Ni(1)− groups (Figure 4). The shortest interchain metal---metal distance is 7.28 Å for Cr3---Ni1. The free $[Cr(CN)_6]^{3-}$ anions are situated in the vicinity of the branched chains (see Supporting Information).

The structure of $[NiL^3]_3[Cr(CN)_5(NO)]_2 \cdot 8H_2O$ (**3**) is similar to that of the 2D honeycomblike layered structures reported previously.[16−21] Like other honeycomblike Ni_3Cr_2 or Ni_3Fe_2 complexes, each $[Cr(CN)_5(NO)]^{3-}$ unit is coordinated to three $[NiL^3]^{2+}$ cations with C_3 rotational symmetry-related three *cis*-C≡N groups, the remaining CN^- and NO^+ groups are monodentate (Figure 5). The C_3 rotational axis at Cr(I) results in the disorder of NO by about three coordination positions with the corresponding Cr−N and Cr−C bond lengths statistically averaged to be 1.920(7) Å. Unlike other honeycomblike Ni_3Cr_2 species, the macrocyclic ligands in the present complex exhibit disorder. Therefore, there are two sets of L^3 around Ni(II) with the dihedral angle of 12.6°.

All the pendant arms of hydroxyethyl are located in the honeycomblike channel formed by Cr−C≡N−Ni linkages. In each honeycomb, all the six hydroxyethyl oxygen atoms are involved in the formation of $O_{water} \cdots O_{hydroxyethyl}$ hydrogen bonds with two O_{water} atoms. In each channel, six O_{water} atoms connected the adjacent two layers by $O_{water} \cdots O_{hydroxyethyl}$ hydrogen bonds leading to a 3D network structure and a cage of O atoms was formed. There are also $O_{water} \cdots O_{water}$ hydrogen bonds in the molecules.

Magnetic Properties. The temperature dependence of the $\chi_m T$ product/NiCr unit in the range 5−150 K for $[Ni(H_2L^2)][Cr(CN)_5(NO)]ClO_4 \cdot 5H_2O$ (**1**) in an applied field of 5 kOe is shown in Figure 6. The $\chi_m T$ value increases smoothly until 5.0 K. The magnetic susceptibility obeys the Curie−Weiss law with a positive Weiss constant $\Theta = +4.8$ K. This behavior is consistent with an intrachain Ni(II)−Cr(I) ferromagnetic interaction, which can be accounted for by the orthogonality of the magnetic orbitals of the metal ions.[21,30a] To evaluate the strength of the intermetallic exchange constants of **1**, we used an approximate approach similar to that previously used for 1D, 2D, and quasi-2D complexes.[24,31] On the basis of the crystal data, the Cr−CN−Ni likages were unequal. Therefore, the 1D chain can be treated as alternating uniform CrNi dimers with the different intradimeric and intrachain exchange constants (J_d vs J_c):

(30) (a) Kou, H.-Z.; Gao, S.; Ma, B.-Q.; Liao, D.-Z. *Chem. Commun.* **2000**, 713. (b) Enemark, J. H.; Quinby, M. S.; Reed, L. L.; Steuck, M. J.; Walthers, K. K. *Inorg. Chem.* **1970**, *9*, 2397.

(31) Chiari, B.; Cinti, A.; Piovesana, O.; Zanazzi, P. F. *Inorg. Chem.* **1995**, *34*, 2652. Burla, M. C.; Chiari, B.; Cinti, A.; Piovesana, O. *Mol. Cryst. Liq. Cryst.* **1995**, *273*, 211. Caneschi, A.; Gatteschi, D.; Melandri, M. C.; Rey, P.; Sessoli, R. *Inorg. Chem.* **1990**, *29*, 4228. Wrzeszcz, G.; Dobrzan'ska, L.; Wojtczak, A.; Grodzicki, A. *J. Chem. Soc., Dalton Trans.* **2002**, 2862.

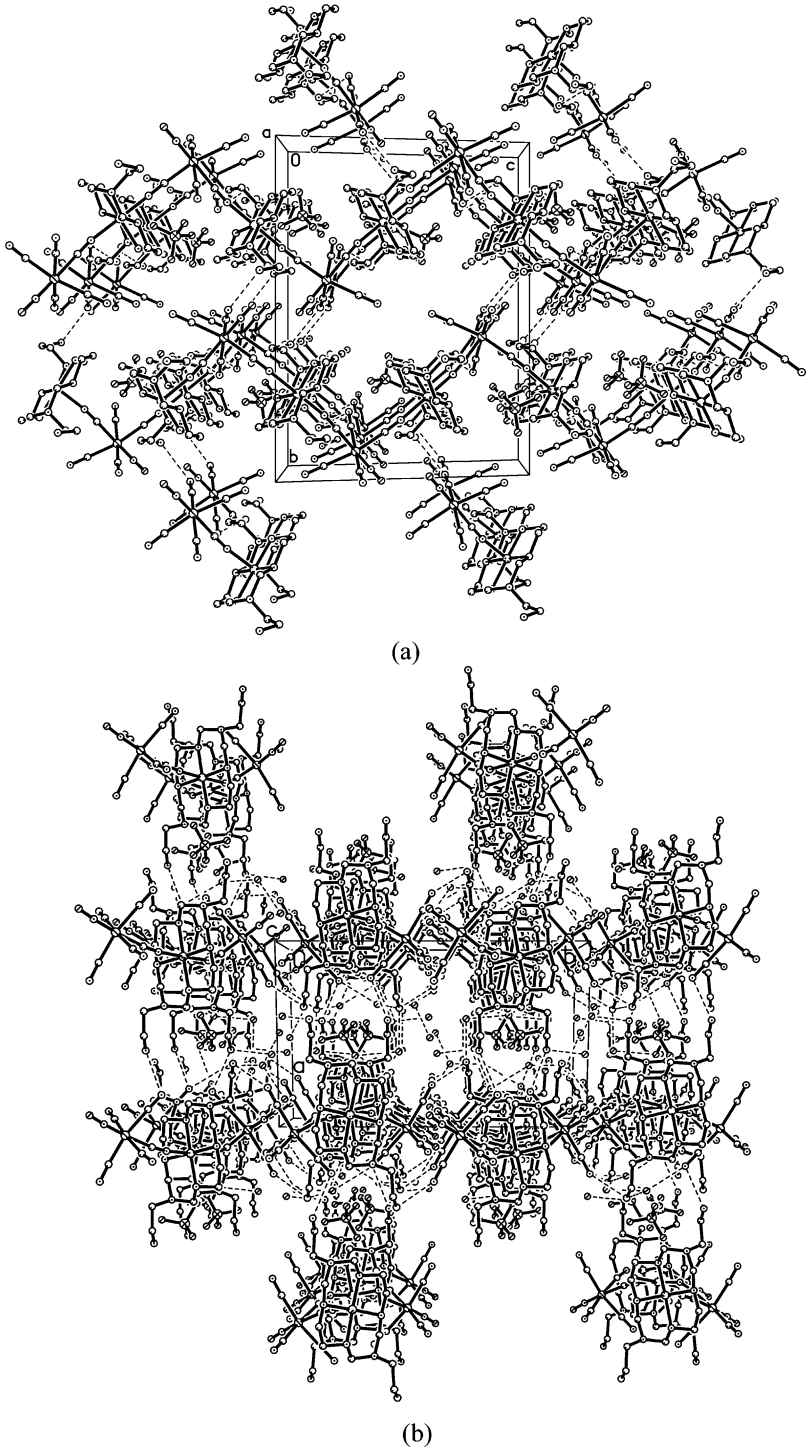

Figure 2. Interchain interaction for **1**: (a) along the *a* axis; (b) along the *c* axis.

$$\chi_d = \frac{Ng^2\beta^2}{4kT}\frac{10 + \exp(-3J_d/kT)}{3 + \exp(5J_d/kT)} \quad (1)$$

$$\chi_d = \frac{Ng^2\beta^2}{3kT}S_d(S_d + 1) \quad (2)$$

$$\chi_{chain} = \frac{Ng^2\beta^2}{3kT}\frac{1 + u}{1 - u}S_d(S_d + 1) \quad (3)$$

Here $u = \coth(J_cS_d(S_d + 1)/kT) - kT/J_cS_d(S_d + 1)$.

Using this rough model, the susceptibility was simulated giving the best fit with parameters $J_c = +0.23$ cm^{-1}, $J_d = +8.4$ cm^{-1}, and $g = 2.05$. The $Ni^{II}-Cr^{I}$ exchange coupling parameter is comparable to that of the cyano-bridged pentanuclear $[Ni(bpm)_2]_3[Fe(CN)_6]_2\cdot 7H_2O$ (bpm = bis(1-pyrazolyl)methane, $J = +5$ cm^{-1}) and $[K(18\text{-C-6})(H_2O)_2][Ni(H_2L)]_2[Fe(CN)_6]_3\cdot 4(18\text{-C-6})\cdot 20H_2O$ (18-C-6 = 18-crown-6-ether, $J = +2.1$ cm^{-1}).[2,23] The J_d value might be attributed to the more linear C≡N−Ni linkages, which has a favorable effect in magnetic interaction.

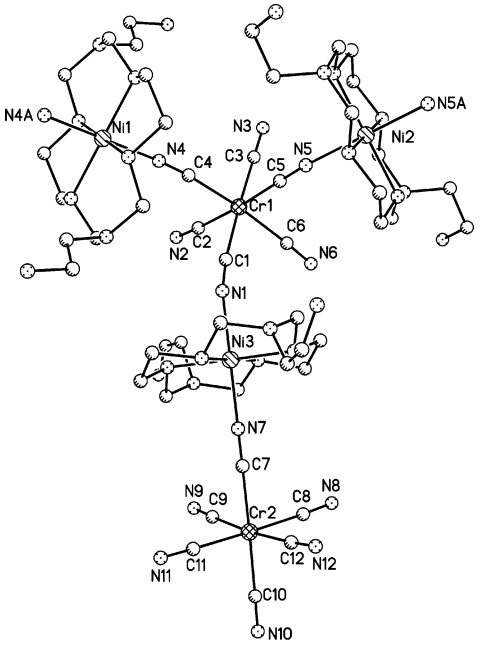

Figure 3. Structure of complex **2**.

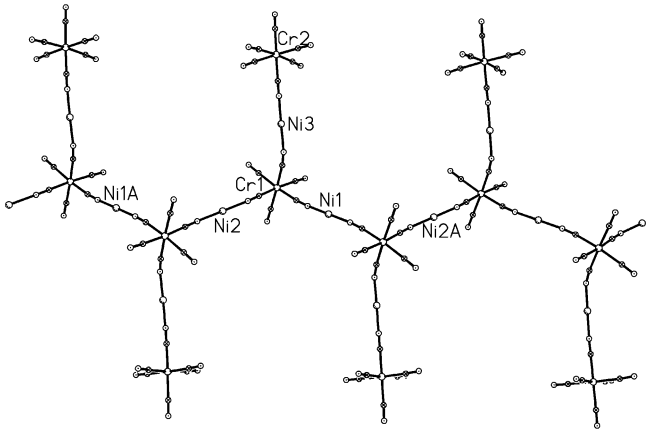

Figure 4. View of the branched chain structure of **2**. The macrocyclic ligands around Ni(II) are omitted for clarity.

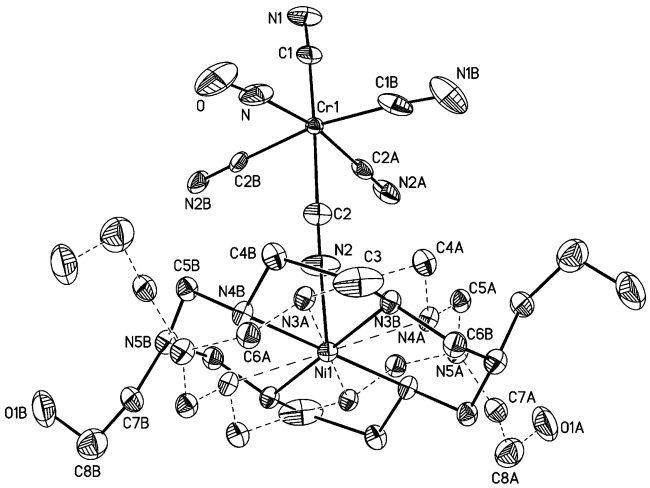

Figure 5. ORTEP drawing of $[NiL]_3[Cr(CN)_5(NO)]_2 \cdot 8H_2O$ (**3**) showing the disorder of the macrocyclic ligand. (Water molecules are not shown.)

The field dependence of the magnetization (0−50 kOe) of **1** measured at 5.0 K shows the gradual increase of the magnetization reaching 1.8 μ_B. The magnetization value at the highest field (50 kOe) is lower than the expected value of 3.0 μ_B for ferromagnetic NiCr. The experimental curves (<30 kOe) lie above the Brillouin curve corresponding to noninteracting one S_{Ni} and one S_{Cr} spins, suggesting the presence of intermetallic ferromagnetic coupling (inset of Figure 6). This indicates the $S = 3/2$ ground state for the complex. The high-field data are low, which may be due to the zero-field-splitting effect of the $S = 3/2$ spin state.

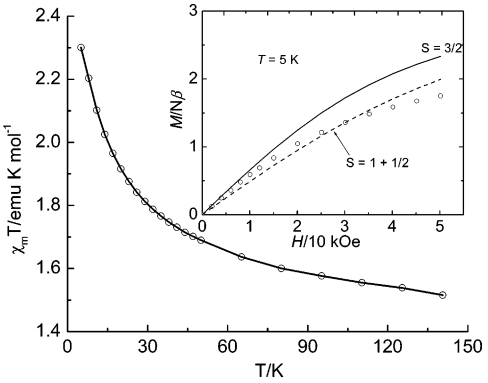

Figure 6. Plot of $\chi_M T$ vs temperature for **1**. The solid line represents the theoretical values on the basis of the parameters described in the text. Inset: field dependence of magnetization at 5 K. The lines represent the Brillouin function that corresponds to noninteracting $S = S_{Ni} + S_{Cr}$ (dashed) and $S = 3/2$ (solid) with $g = 2.0$.

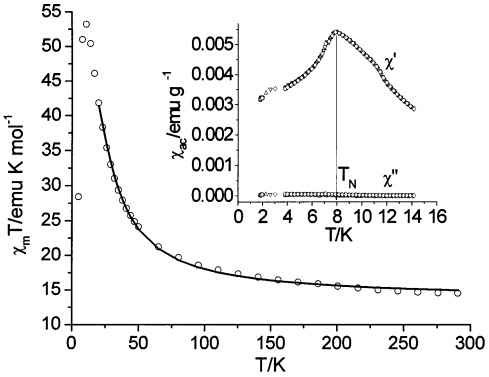

Figure 7. Plot of $\chi_M T$ vs temperature for **2**. The solid line represents the theoretical values on the basis of the parameters described in the text. Inset: temperature dependence of ac magnetization in zero-static field and an ac field of 2 Oe at frequencies of 111, 199, 355, 633, and 1111 Hz.

The magnetic susceptibilities of $[Ni(H_2L^2)]_4[Cr(CN)_6]_5OH \cdot 15H_2O$ (**2**) have been measured on a SQUID magnetometer in the temperature range 5.0−290 K. A plot of $\chi_m T$ vs. T for **2** is shown in Figure 7, where χ_m is the magnetic susceptibility/Ni_4Cr_5 unit. With the decrease of the temperature $\chi_m T$ increases smoothly reaching a maximum value of 53.2 emu K mol^{-1} at 11 K and then decreases, which indicates the presence of ferromagnetic coupling within the chain and interchain antiferromagnetic interaction and the zero-field-splitting effect of the Ni(II) ions. The magnetic susceptibility above 50 K obeys the Curie−Weiss law with a positive Weiss constant $\Theta = +26.4$ K, which also proves the presence of a global ferromagnetic behavior of the complex.

Using an approximate approach similar to that for complex **1**, we tried to estimate the magnitude of the $Cr^{III}-Ni^{II}$ magnetic exchange.[31] The Cr−CN−Ni linkages were considered equivalent for simplicity. On this basis, the 1D chain

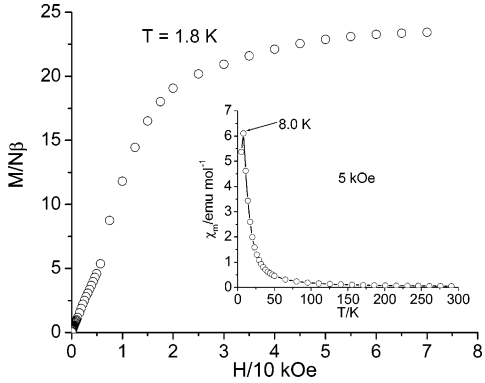

Figure 8. Field dependence of magnetization for **2** at 1.8 K. Inset: FCM of **2** in an applied field of 5 kOe. (The line is a guide for the eye.)

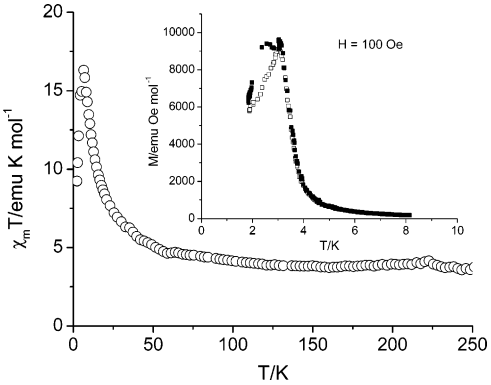

Figure 9. Temperature dependence of $\chi_m T$ for **3** measured at 10 kOe. Inset: FCM (□) and ZFCM (■) of **3** in an applied field of 100 Oe.

can be treated as alternating Cr_2Ni trimers and Ni(II) ions with identical $Ni^{II}-Cr^{III}$ coupling constants (J_{CrNi}):

$$\chi_t = \frac{Ng_t^2\beta^2}{3kT}S_t(S_t+1) \quad (4)$$

$$\chi_{chain} = \frac{4N\beta^2}{3kT}\left[\bar{g}^2\frac{1+u}{1-u} + \delta^2\frac{1-u}{1+u}\right]$$

$$\bar{g} = [g_t\sqrt{S_t(S_t+1)} + g_{Ni}\sqrt{S_{Ni}(S_{Ni}+1)}]/2 \quad (5)$$

$$\delta = [g_t\sqrt{S_t(S_t+1)} - g_{Ni}\sqrt{S_{Ni}(S_{Ni}+1)}]/2$$

$$u = \coth(J_e/kT) - kT/J_e \quad J_e = J\sqrt{S_t(S_t+1)S_{Ni}(S_i+1)}$$

$$\chi_M = 2\frac{\chi_{chain}}{1-\chi_{chain}(2zJ'/Ng^2\beta^2)} + \frac{Ng_{Cr}^2\beta^2}{3kT}S_{Cr}(S_{Cr}+1) \quad (6)$$

Using this model, the susceptibility above 20 K was simulated by eqs 4−6,[32] where S_t is the effective spin of the Cr_2Ni trimer and J_t and J_c are the coupling constants of the trimer and the chain, respectively. The best fit to the experimental data gives the parameters $J_{CrNi} = J_t = J_c = +5.9(1)$ cm^{-1}, $g = g_t = g_{Cr} = g_{Ni} = 2.02(1)$, and $zJ' = -0.20(1)$ cm^{-1}. The data below 20 K could not be satisfactorily fitted. The $Ni^{II}-Cr^{III}$ exchange coupling parameter is comparable to that of the cyano-bridged $Ni^{II}Cr^{III}$ clusters.[33−35]

Interestingly, magnetic susceptibility measurements of the zero-static field ac magnetic susceptibilities at different frequencies confirm the antiferromagnetic ordering below 8.0 K (inset of Figure 7). The field dependence of magnetization shows the metamagnetic behavior at 1.8 K (Figure 8): first M increases linearly with the increase of H until 6 kOe and then increases abruptly. This indicates that the critical field (the lowest field which is used to reverse the antiferromagnetic interaction) is approximately 6 kOe at 1.8 K. The metamagnetic behavior is also confirmed by FCM measurements in an applied field of 5 kOe. As shown in the inset of Figure 8, a maximum is observed at 8.0 K, suggesting that the critical field is larger than 5 kOe. The magnetization saturates above 60 kOe, reaching 23.4 μ_B (expected value: 23 μ_B for $S_T = 23/2$). Compared with the 2D honeycomblike $Ni^{II}_3Cr^{III}_2$ complexes that order antiferromagnetically below 15 K,[16,18,20,21] the T_N value of 8.0 K for the 1D complex (**2**) is high, which is due to the presence of very strong interchain antiferromagnetic interaction in the complex.[36]

Figure 9 shows the magnetic susceptibilities of $[NiL^3]_3[Cr(CN)_5(NO)]_2\cdot 8H_2O$ (**3**) in the form of $\chi_m T$ vs T per Ni_3Cr_2 unit. The $\chi_m T$ value increases gradually down to ca. 50 K and then sharply reaches a maximum value of 16.3 emu K mol^{-1} (11.4 μ_B) at 6.5 K. The $\chi_m T$ value decreases abruptly below 6.5 K and reaches a value of 9.24 emu K mol^{-1} (8.6 μ_B) at 2.3 K, which is due to the interlayer antiferromagnetic interactions and/or the saturation effect. The magnetic susceptibility above 15 K obeys the Curie−Weiss law with a positive Weiss constant Θ of +13.0 K and the Curie constant of 3.58 emu K mol^{-1}, which is similar to the calculated value of 3.75 emu K mol^{-1} ($g = 2.0$). The field-cooled magnetization vs temperature plot (inset of Figure 9) with the applied field $H = 100$ Oe shows a break at ca. 3 K, which demonstrates that there exists an antiferromagnetic phase transition at ca. 3 K.

The magnetic phase transition is further confirmed by the temperature dependence at zero dc and 5 Oe ac field susceptibility measurements displayed in Figure 10. The real part of the ac magnetic susceptibility has a maximum peak at about 3.3 K, suggesting that the critical temperature (T_N) can be estimated at 3.3 K. The frequency dependence of χ_{ac}' and χ_{ac}'' suggests a degree of glassy behavior, which may be related to the disorder of the macrocyclic ligands in the crystal lattice. The appearance of a weak χ_{ac}'' signal suggests that the magnetic ordering should be a ferromagnetic order; however, this supposition was excluded on the basis of further magnetic characterizations.

(32) Drillon, M.; Coronado, E.; Beltran, D.; Georges, R. *Chem. Phys*. **1983**, *79*, 449.
(33) Marvilliers, A.; Pei, Y.; Boquera, J. C.; Vostrikova, K. E.; Paulsen, C.; Rivière, E.; Audière, J.-P.; Mallah, T. *Chem. Commun*. **1999**, 1951.
(34) Mallah, T.; Auberger, C.; Verdaguer, M.; Veillet, P. *J. Chem. Soc., Chem. Commun*. **1995**, 61.
(35) Berseth, P. A.; Sokol, J. J.; Shores, M. P.; Heinrich, J. L.; Long, J. R. *J. Am. Chem. Soc*. **2000**, *122*, 9655.
(36) We are indebted to one reviewer for drawing our attention to the fact that the intermolecular hydrogen bonding in low-dimensional species is not the only factor causing a 3D magnetic order. See the following: Berlinguette, C. P.; Gala'n-Mascaro's, J. R.; Dunbar, K. R. *Inorg. Chem*. **2003**, *42*, 3416.

Table 5. Comparison of Structures and Magnetic Properties of 2D Ni_3M_2 Complexes

compd	Ni−$N_{cyanide}$/Å	Ni···M[a]/Å	T_N or T_c/K	ref
$[Ni(cyclam)]_3[Cr(CN)_6]_2\cdot 20H_2O$	2.06(2)−2.12(1)	8.06−8.1 6	<2	16
$[NiL^3]_3[Cr(CN)_6]_2\cdot 18H_2O$	2.087(3)	7.773	12.6 (T_N)	18
$[NiL^4]_3[Cr(CN)_6]_2\cdot 7H_2O$	2.100(4)−2.143(3)	6.953	13 (T_N)	21
$[NiL^5]_3[Cr(CN)_6]_2\cdot 18H_2O$	2.089(10)	unknown	14 (T_N)	20
$[NiL^1]_3[Cr(CN)_6]_2\cdot 9H_2O$	2.094(4)	7.822	11.9 (T_N)	21
$[NiL^3]_3[Fe(CN)_6]_2\cdot 8H_2O$	2.083(7)	7.784	6.0 (T_N)	19b
$[NiL^4]_3[Fe(CN)_6]_2\cdot 9H_2O$	2.088(9)	7.706	5.1 (T_N)	19a
$[NiL^5]_3[Fe(CN)_6]_2\cdot 22.5H_2O$	2.123(3)−2.144(3)	7.688	8.0 (T_N)	17
$[NiL^3]_3[Cr(CN)_5(NO)]_2\cdot 8H_2O$	2.063(4)	7.564	3.3 (T_N)	this work
$[NiL^1]_3[Cr(CN)_5(NO)]_2\cdot 9H_2O$	2.080(3)	7.647	4.3 (T_C)	21
$[NiL^4]_3[Cr(CN)_5(NO)]_2\cdot 10H_2O$	2.153(3)	6.910	4.5 (T_C)	30a

[a] Nearest metal−metal interlayer distance. L^5 = 1,4,8,11-tetramethyl-1,4,8,11-tetraazacyclotetradecane.

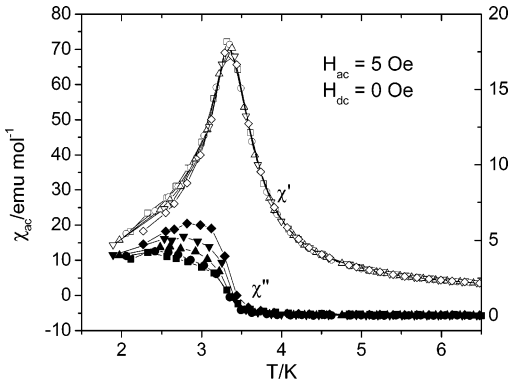

Figure 10. Temperature dependence of zero-static field ac magnetic susceptibilities for **3** measured at frequencies of 111 (□♀ ■), 199 (○♀ ●), 355 (△♀ ▲), 633 (▽♀ ▼), 1111 Hz (◇♀ ◆).

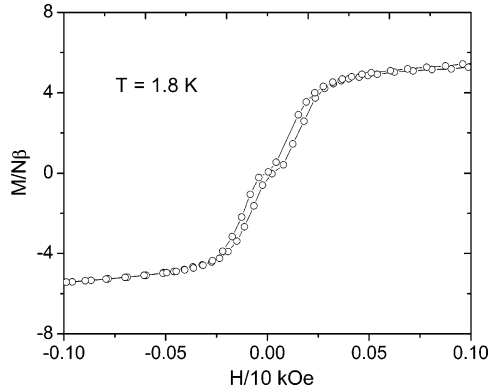

Figure 11. Magnetic hysteresis loop at 1.8 K for **3**.

The hysteresis loop at 1.8 K (Figure 11) shows that the increasing speed of magnetization with the increasing of magnetic field changes from slow to fast, indicating a spin-flip from antiferromagnetic to ferromagnetic arrangement between the layers. A maximum coercive field of 40 Oe is observed in the ferromagnetic state. This metamagnetic behavior is commonly observed for the 2D layered antiferromagnets with short-range intralayer ferri- or ferromagnetic ordering.[17−21]

The field dependence of the magnetization (0−50 kOe) at 1.8 K shows rapid saturation of magnetization value reaching 7.86 $N\beta$ at 50 kOe, close to the expected value of 8 $N\beta$ for a ferromagnetic Ni_3Cr_2 species.

It is known that, in the 2D Ni_3Fe_2 bimetallic antiferromagnets, longer Ni−$N_{cyanide}$ and Ni···Fe *interlayer* distances lead to lower T_N values because of the weaker *intralayer* ferromagnetic coupling and *interlayer* antiferromagnetic interactions. With several similar 2D honeycomblike Ni_3M_2 [M = Fe(III), Cr(III), Cr(I)] available systems (Table 5), it is useful to compare the magnetism of these complexes. For isostructural Cr(III) and Cr(I) antiferromagnets, the T_N of the former is much higher than that of the latter. This difference can be assigned to the stronger *intralayer* Ni(II)−Cr(III) magnetic coupling and/or the stronger *interlayer* magnetic interaction. The stronger *intralayer* Ni(II)−Cr(III) exchange compared with Ni(II)−Cr(I) interaction is due to the presence of more electrons in Cr(III). For analogous Cr(I) and Fe(III) antiferromagnets,[17,19] due to the same electron configuration of two metal ions, the lower T_N value for the Cr(I) complex can be tentatively attributed to the weaker *interlayer* antiferromagnetic interaction, which can be shown by the comparison of the H_c values of them. Although the Cr(I) analogue possesses comparatively strong intralayer ferromagnetic interaction (higher Weiss constant), the weaker *interlayer* antiferromagnetic coupling results in a lower T_N value. It should be noted that the magnitude of the *interlayer* antiferromagnetic interaction seems not well correlated to the *interlayer* metal---metal separations (Table 5), which indicates the complexity of the magnetic interaction. Therefore, more work is needed to ultimately uncover the magneto−structure relationship.

Acknowledgment. This work was supported by the National Natural Science Foundation of China (Project Nos. 20201008 and 50272034). K.H.Z. thanks Prof. Yadong Li for helpful discussions and for providing excellent working conditions.

Supporting Information Available: Crystal cell packing plots of complexes **2** and **3**, a figure showing the field dependence (0−50 kOe) of magnetization at 1.8 K for **3**, and an X-ray crystallographic CIF file. This material is available free of charge via the Internet at http://pubs.acs.org.

IC034028Y